THE DELFT SYSTEMATIC YACHT HULL SERIES II EXPERIMENTS

Prof.ir. J. Gerritsma, Ir. J.A. Keuning and R. Onnink

Report Nr. 881-P

The Tenth Chesapeake Sailing Yacht Symp.
February 9, 1991

Delft University of Technology
Ship Hydromechanics Laboratory
Mekelweg 2
2628 CD Delft
The Netherlands
Phone 015 - 78 68 82

THE TENTH CHESAPEAKE SAILING YACHT SYMPOSIUM

1991

CSYS

FEBRUARY 9, 1991

THE CHESAPEAKE SECTION
OF
THE SOCIETY OF NAVAL ARCHITECTS
AND
MARINE ENGINEERS

THE CHESAPEAKE BAY
YACHT RACING ASSOCIATION

U.S. NAVAL ACADEMY
SAILING SQUADRON

THE DELFT SYSTEMATIC YACHT HULL SERIES II EXPERIMENTS

Prof. ir. J. Gerritsma, Ir. J.A. Keuning and R. Onnink,
Delft University of Technology, The Netherlands

ABSTRACT

The Delft Systematic Yacht Hull Series (series I) has been extended with six hull forms which cover a range of medium to very light displacements.
Upright and heeled resistance, as well as side force and stability have been measured for a large range of forward speeds.
Polynomial expressions for the upright resistance, based on the combined Series I and II, are given for Froude numbers up to Fn = 0.60.
The measured side force and induced resistance are analysed, and velocity predictions using Series I and II results are discussed.

NOMENCLATURE

A_w	=	waterplane area	m^2
A_R	=	aspect ratio	
A_k	=	projected keel area	m^2
A_x	=	main cross section area	m^2
BAD	=	boom above deck	m
B_{max}	=	maximum breath	m
B_{wl}	=	waterline breath	m
C_f	=	frictional resistance coefficient	
C_p	=	prismatic coefficient	
E	=	boom length	m
Fn	=	Froude number	
F_h	=	side force	N
FMI	=	freeboard measured at mast	m
g	=	acceleration due to gravity	m/s^2
G	=	centre of gravity	
GM	=	metacentric height	m
I	=	fore triangle height	m
J	=	fore triangle base length	m
L_{wl}	=	waterline length	m
LCB	=	longitudinal position of centre of buoyancy	$\%L_{wl}$
P	=	mainsail hoist	m
q	=	$\frac{1}{2}\rho V^2$	kg/ms^2
R_φ	=	total resistance with heel and leeway	N
R_f	=	frictional resistance	N
RM	=	righting moment 1^o degree heel	Nm
R_r	=	residuary resistance	N
R_t	=	total upright resistance	N
Rn	=	Reynolds number	
S	=	wetted area	m^2
S_A	=	sail area	m^2
S_c	=	wetted area canoe body	m^2
S_k	=	wetted area keel	m^2
S_r	=	wetted area rudder	m^2
T	=	total depth	m
T_c	=	depth canoe body	m
V	=	speed	m/s
β	=	leeway angle	radians
Δ	=	weight of displacement	N
∇	=	volume of displacement	m^3
φ	=	heel angle	radians
ρ	=	specific density	kg/m^3

INTRODUCTION

In view of the recent trend in yacht design to light displacement hull forms, the Delft Systematic Yacht Hull Series has been extended with six hull forms.
Because of the higher speed potential of light displacement yachts, dynamic lift effects have to be considered and yacht speeds exceeding Fn = 0.45, which corresponds to the speed limit of the original Series I, are now important. Therefore, the Series II six models were tested for speeds up to Fn = 0.725, exceeding the "hull speed" by approximately 80% in some cases.
For VPP purposes a new regression model for the upright resistance of Series I (the original Series) + Series II (the

six additional hull forms) has been derived from the model experiment results, for speeds up to Fn = 0.45.
Based on the Series II results, a separate regression model for the range of speeds corresponding to Fn = 0.45 to 0.60 has been developed.
In general, the Series II hull forms are characterized by more flat sections, as compared with Series I. In particular, some very large beam/draught ratios of the canoe body are represented in Series II.
The same keel and rudder geometry as for Series I was used to avoid, as far as possible, the influence of differences due to the keel-rudder arrangement. Although this led to somewhat unrealistic keel-hull combinations, in particular in case of the very large beam/draught ratios, this was accepted in view of the matching of the Series I and II experimental results.
The Series II models were tested with heel and leeway. The measured side force and heeled resistance are analysed in the same way as for Series I [1].

The performance of light-displacement yachts shows some interesting differences when compared with that of medium and heavy displacement yachts. With the results of Series I and Series II, velocity predictions have been made for yacht hull forms which differ considerably in their length-displacement ratio. The comparison also includes the influence of stability on sailing performance.

GEOMETRY OF THE SERIES II HULL FORMS

The six models have been derived from one parent form, developed in cooperation with E.G. van de Stadt & Partners bv. The body plans of the parent forms of Series I and Series II are given in Figure 1 to show the considerable differences in section shape. The Series II parent hull form has a more flat bottom than does the Series I parent; the main section coefficients A_x are respectively 0.70 and 0.65.
In Figure 2a, b and c, the buttocks, sections and waterlines of the six Series II hull forms, numbered 23-28, are depicted. Model 25 is the parent form.
All the Series II models have an almost equal prismatic coefficient (C_p = 0.55) and an equal longitudinal position of the centre of buoyancy (LCB = 2% of L_{Wl} aft of midships), but the length-displacement ratio varies ($L_{Wl}/\nabla_c^{1/3}$ = 5 to 8). The length/beam ratio at the designed waterline varies from 3.5 to 4.5 and the beam/draught at the main cross section varies from 2.4 to 10.5.

In Table 1, the main dimensions and some other geometric particulars of the Series II hull forms are given, based on a waterline length, L_{Wl}, of 10 meters.

In Table 2, the main hull form parameters are summarized.

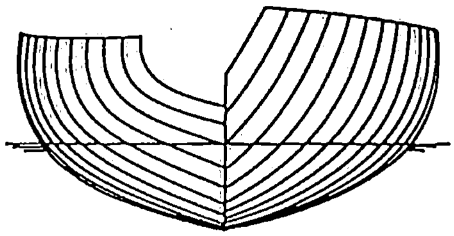

PARENT MODEL SERIES I

$L/\Delta^{1/3}$ = 4.78

L_{WL}/B_{WL} = 3.17

B_{WL}/T_c = 4.01

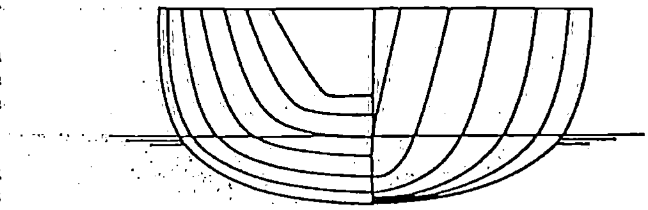

PARENT MODEL SERIES II

$L/\Delta^{1/3}$ = 6.0

L_{WL}/B_{WL} = 4.0

B_{WL}/T_c = 5.2

Figure 1. Parent model Delft Series I and Delft Series II.

TABLE 1

Main dimensions and derived quantities

model nr.	L_{wl} m	B_{max} m	B_{wl} m	T_c m	T m	∇_c m^3	S_c m^2	A_x m^2	A_w m^2
23	10.00	3.20	2.86	0.704	1.80	7.974	23.32	1.46	19.3
24	10.00	3.30	2.86	0.261	1.36	2.895	19.85	0.55	19.0
25	10.00	2.80	2.50	0.464	1.56	4.618	18.98	0.84	16.7
26	10.00	2.90	2.50	0.194	1.29	1.972	17.30	0.36	16.7
27	10.00	2.50	2.22	0.904	2.00	7.915	21.73	1.44	14.9
28	10.00	2.55	2.22	0.329	1.43	2.922	16.17	0.54	14.6

TABLE 2

Main hull form parameters

model nr.	L_{wl}/B_{wl}	B_{wl}/T_c	C_p	$L_{wl}/\nabla_c^{1/3}$	LCB (%)	$A_w/\nabla_c^{2/3}$
23	3.50	4.06	0.55	5.00	-1.9	4.84
24	3.50	10.96	0.55	6.93	-2.1	9.14
25	4.00	5.39	0.55	6.01	-1.9	6.02
26	4.00	12.89	0.55	7.97	-2.1	10.82
27	4.50	2.46	0.55	5.02	-1.9	3.75
28	4.50	6.75	0.55	6.89	-1.9	7.14

Finally, Table 3 gives the keel and rudder dimensions, also corresponding to a waterline length, L_{Wl}, of 10 meters.

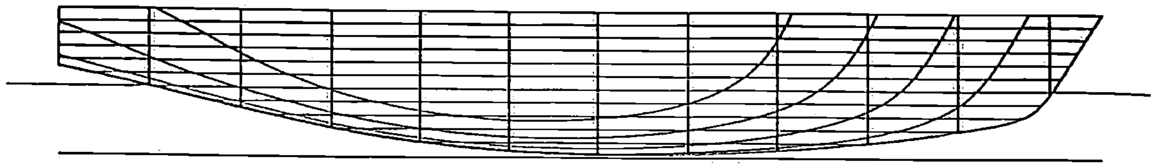

NR.23

L/B = 3.5 $L/\Delta^{1/3} = 5.0$

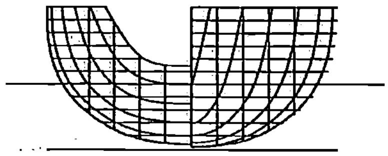

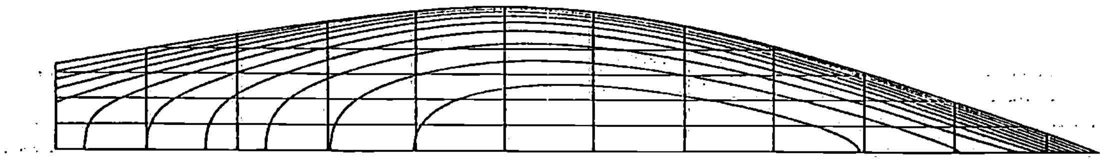

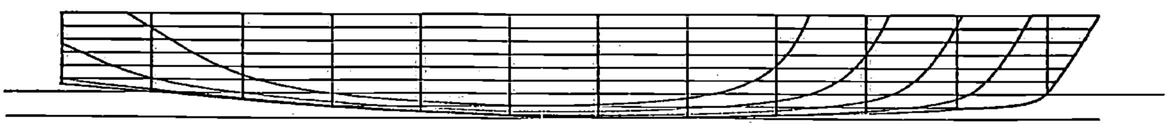

NR.24

L/B = 3.5 $L/\Delta^{1/3} = 7.0$

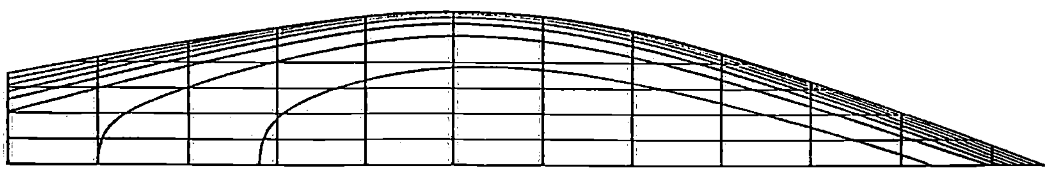

Figure 2a. Lines of Series II.

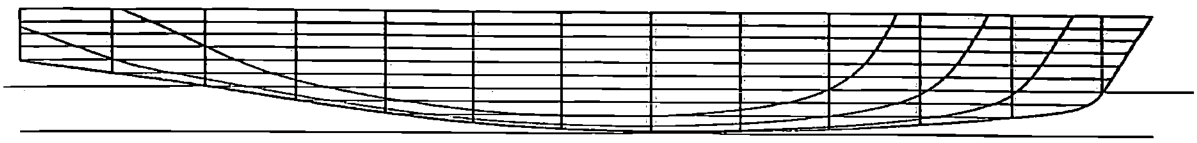

NR.25

L/B = 4.0 $L/\Delta^{1/3} = 6.0$

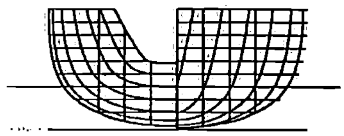

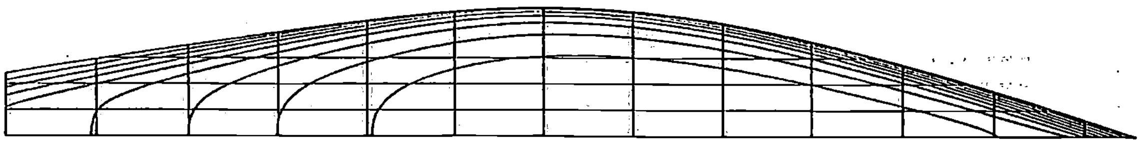

NR.26

L/B = 4.0 $L/\Delta^{1/3} = 8.0$

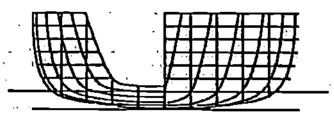

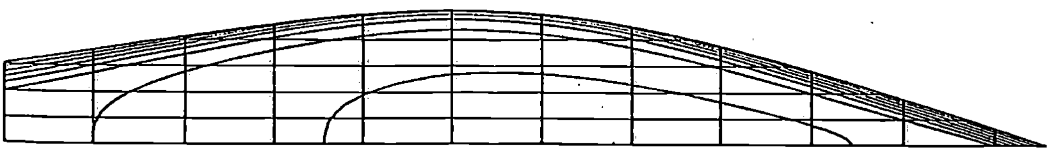

Figure 2b. Lines of Series II.

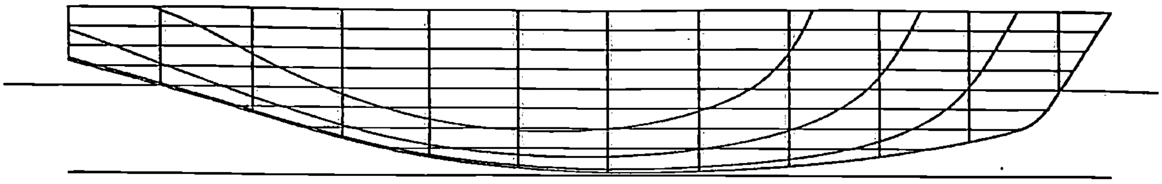

NR.27

$L/B = 4.5$ $L/\Delta^{1/3} = 5.0$

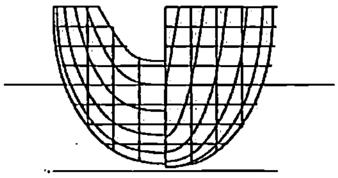

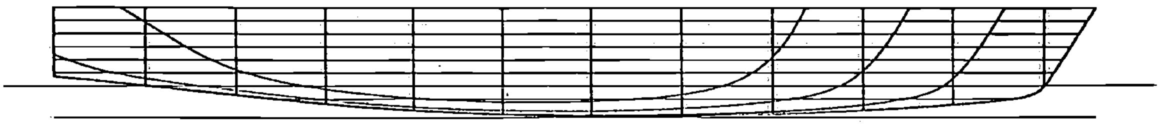

NR.28

$L/B = 4.5$ $L/\Delta^{1/3} = 7.0$

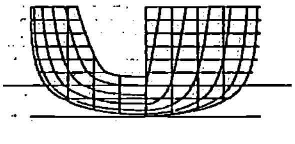

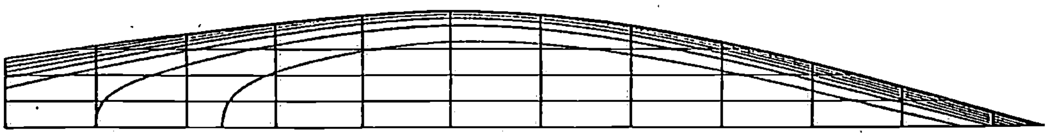

Figure 2c. Lines of Series II.

TABLE 3

Keel and rudder dimensions

	volume m^3	wetted area m^2	root chord m	tip chord m	span m
keel	0.327	3.85	2.07	1.31	1.10
rudder	0.028	1.38	0.82	0.48	1.33

Keel and rudder profiles are, respectively, NACA 63A015 and 0012. The fin keel and rudder arrangement, which is uniform for the six hull forms considered, is depicted in Figure 3.

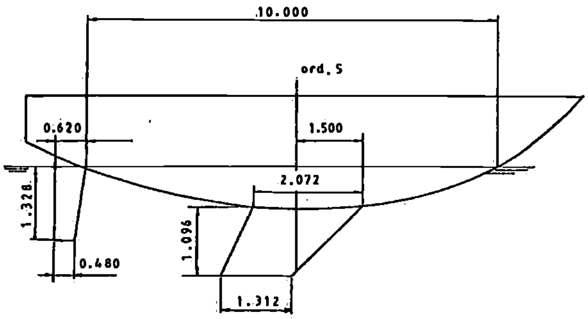

Keel profile NACA 63 A 015
Rudder ,, NACA 0012

Figure 3. Keel - Rudder arrangement of Series II; L_{Wl} = 10 meter.

The ranges of the hull form parameter values, now covered by the twenty-eight models of the combined Series I and II, are shown in Figure 4. The large extensions of the ranges of the beam/draught ratio and the length-displacement ratio are clearly demonstrated in this figure.

RESISTANCE EXPERIMENTS

Experimental setup

Glass fibre reinforced polyester models with an overall length, L_{oa}, of 2.3 meters and a waterline length, L_{Wl}, of 2.0 meters have been used to carry out resistance and side force experiments in the Nr.1 Towing Tank of the Delft Ship Hydromechanics Laboratory.
The turbulence stimulation consists of widely spaced carborundum grains, Size 20, with a density of approximately 10 grains per cm², as described in reference [1].
Measured model resistances have been corrected for the resistance increase due to the turbulence stimulation.
No blockage corrections have been applied to the measured resistance values, the maximum ratio of the model main cross section area, A_x, and the wetted cross-section of Tank Nr.1 being smaller than 0.5%.
The test arrangement to measure resistance and side force with heel and leeway was similar to that used for the Series I experiments [1].

Upright resistance

In Table 4 the residuary resistance,

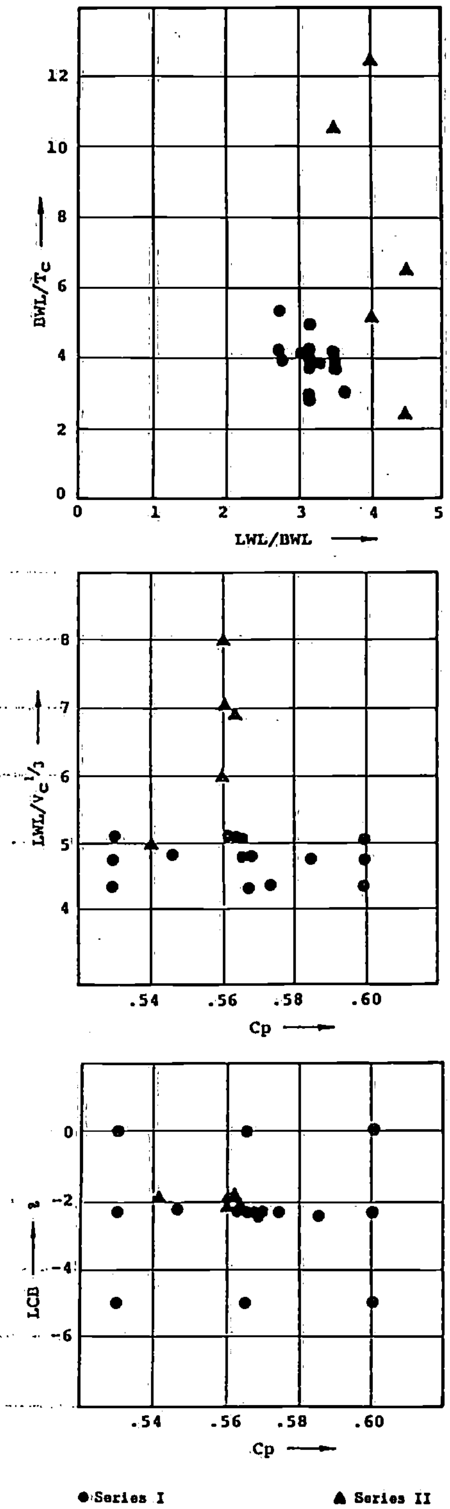

Figure 4. Form parameters of Series I and II.

R_r, per unit weight of displacement of the canoe body, ∇_c, is given for Froude nr values from 0.125 to 0.750 where:

$$Fn = V/\sqrt{(g * L_{Wl})}$$

The residuary resistance has been determined with:

$$R_r = R_t - R_f \qquad (1)$$

where:

R_t - the measured total upright resistance

R_f - the frictional resistance component according to the 1957 ITTC C_f formulation:

$$C_f = 0.075/(\log Rn - 2)^2 \qquad (2)$$

$$Rn = V * (0.7\ L_{wl})/\nu$$

TABLE 4

Residuary resistance per unit weight of displacement of the canoe body. $R_r/\nabla * 10^3$

	Model					
Fn	23	24	25	26	27	28
0.125	0.01	-	-	-	-	-
0.150	0.26	-	-	0.75	0.04	-
0.175	0.38	0.99	0.78	1.79	0.15	1.05
0.200	0.59	1.70	1.27	1.04	0.38	1.23
0.225	0.88	1.93	1.46	2.12	0.56	1.56
0.250	1.25	3.42	2.61	3.07	0.94	2.03
0.275	2.03	3.65	2.81	3.74	1.58	3.15
0.300	2.89	4.81	3.72	4.63	2.15	3.77
0.325	4.16	6.36	5.08	7.29	3.25	5.54
0.350	8.17	9.50	7.74	9.88	5.62	7.72
0.375	11.29	14.25	12.75	13.50	11.83	12.60
0.400	20.98	21.63	20.70	20.64	21.77	20.04
0.425	34.28	30.86	31.58	28.98	34.96	30.39
0.450	49.47	41.23	44.03	38.31	49.52	38.87
0.475	63.87	48.85	54.21	44.91	63.06	46.19
0.500	81.60	56.32	63.91	52.85	-	53.85
0.525	94.38	63.46	72.62	58.43	-	59.74
0.550	104.97	69.63	79.56	63.74	-	65.47
0.575	-	75.49	85.84	68.84	-	70.18
0.600	-	80.85	92.17	75.03	-	74.98
0.625	-	85.24	97.74	78.60	-	79.68
0.650	-	89.02	101.67	82.95	-	84.64
0.675	-	91.21	-	87.79	-	90.39
0.700	-	-	-	91.99	-	96.40
0.750	-	-	-	96.50	-	102.72

The separate contributions of hull, keel and rudder to R_r have been added, using 70% of the L_{wl} as the length in the computation of Rn for the hull and the mean chord lengths for computation of keel and rudder Rn values; thus,

$$R_f = \tfrac{1}{2}\rho V^2 (S_c * C_{fc} + S_k * C_{fk} + S_r * C_{fr}) \qquad (3)$$

where S_c, S_k and S_r are the wetted areas of the canoe body, keel and rudder, respectively, and the coefficients C_f are the corresponding frictional resistance coefficients.

A new polynomial expression for the residuary resistance for speeds up to those corresponding to Fn = 0.45 has been derived from the results of all the 28 models of Series I and II. For the speed range corresponding to Fn = 0.45 to 0.60, a separate expression based on the Series II results has been derived.

The regression models for the two speed ranges are as follows:

for Fn = 0.125 to 0.450:

$$R_r/\Delta_c * 10^3 = A0 + A1(C_p) + A2(LCB) + A3(B_{wl}/T_c) + A4(L_{wl}/\nabla_c^{1/3}) + A5(C_p)^2 + A6(C_p * L_{wl}/\nabla_c^{1/3}) + A7(LCB)^2 + A8(L_{wl}/\nabla_c^{1/3})^2 + A9(L_{wl}/\nabla_c^{1/3})^3 \qquad (4)$$

for Fn = 0.45 to 0.60:

$$R_r/\Delta_c * 10^3 = C0 + C1(L_{wl}/B_{wl}) + C2(A_w/\nabla_c^{2/3}) + C3(L_{wl}/B_{wl})^2 + C4(L_{wl}/B_{wl}) * (A_w/\nabla_c^{2/3})^3 \qquad (5)$$

where:

∇_c = volume of displacement of the canoe body

$\Delta_c = \rho g \nabla_c$

= weight of displacement of the canoe body

The coefficients A and C of Expressions (4) and (5) are listed in the Tables 5 and 6.

It should be noted that in Expression (5), the form parameter $A_w/\nabla_c^{2/3}$ has been included. This parameter can be regarded as a load factor of the waterplane area and is frequently used in polynomial expressions for determining the resistance of planing boats. A large value of $A_w/\nabla_c^{2/3}$ could indicate an important dynamic lift component in the high speed range.

The resistance versus speed curve in such a case bears no resemblance to the characteristic steep resistance increase of a medium or heavy displacement hull form when it is exceeding the hull speed; rather a more gradual resistance increase with speed is observed.

The correlation between the experimental values and the regression model is very satisfactory. In particular, in the speed range corresponding to Fn = 0.45 to 0.60, the predicted resistance, as based on only two form parameters, L_{wl}/B_{wl} and $A_w/\nabla_c^{2/3}$, and the weight of displacement Δ_c, is very close to the experimental values. In Figure 5 the predicted total upright resistance is compared with the measured values for Models 25 and 26, as examples.

As shown in Table 2, the six models have an almost equal longitudinal position of the centre of buoyancy. It should be noted that a different L_{CB} could influence the predicted resistance to some extent. The influence of L_{CB} will be reported in the near future, as a result of testing an additional series of eleven models (Series III).

Heeled resistance, side force and stability

For each of the six models of series II, experiments have been carried out to

TABLE 5

Residuary resistance polynomial coefficients Fn = 0.125 to 0.450.

Fn	A_0 A_5	A_1 A_6	A_2 A_7	A_3 A_8	A_4 A_9
0.125	-12.45884 -35.64266	+41.96056 -0.557162	-0.015664 -0.003683	+0.054216 +0.063850	+0.172104 -0.006880
0.150	-16.63653 -30.52534	+48.04490 -3.193774	-0.014415 -0.004341	+0.022791 +0.268158	+0.732430 -0.019881
0.175	-5.440638 -28.80142	+27.47384 +1.073305	+0.006670 -0.001053	+0.065666 +0.133609	-1.074351 -0.010561
0.200	+11.67324 -11.58520	-14.97679 +5.792068	+0.047823 +0.007154	+0.085557 -0.093147	-2.774123 +0.006347
0.225	+27.62608 +4.128028	-52.72783 +10.06511	+0.093202 +0.014441	+0.151896 -0.135946	-4.915521 +0.008620
0.250	+41.57053 +15.23234	-84.10490 +14.54537	+0.173649 +0.029416	+0.190659 -0.256058	-6.921805 +0.017730
0.275	+54.77415 +45.43005	-123.9809 +16.84450	+0.225905 +0.039728	+0.254739 -0.267875	-8.101425 +0.017628
0.300	+76.66092 +114.7038	-202.8173 +18.79237	+0.396418 +0.074764	+0.341964 -0.521396	-8.068824 +0.034366
0.325	+137.9019 +302.6570	-417.2575 +20.40004	+0.676888 +0.116017	+0.460046 -0.684892	-8.171168 +0.044301
0.350	+266.8098 +636.3422	-830.7063 +25.85210	+1.154643 +0.180037	+0.541289 -0.767488	-10.72063 +0.047520
0.375	+358.9669 +817.6215	-1095.062 +31.45530	+1.671016 +0.244167	+0.530508 -1.378868	-10.70230 +0.082385
0.400	+537.5134 +1171.654	-1598.655 +45.01871	+1.982948 +0.281434	+0.270975 -1.641891	-16.79936 +0.096662
0.425	+608.3943 +1018.761	-1647.524 +83.67038	+2.273537 +0.332559	+0.025498 -4.570643	-24.20854 +0.277169
0.450	+943.9202 +1643.984	-2651.320 +138.8056	+2.913360 +0.469272	+0.298555 -11.37453	-22.67869 +0.693914

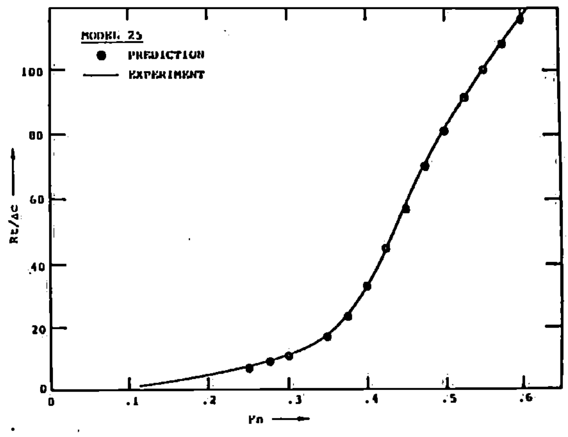

Figure 5a. Total upright resistance

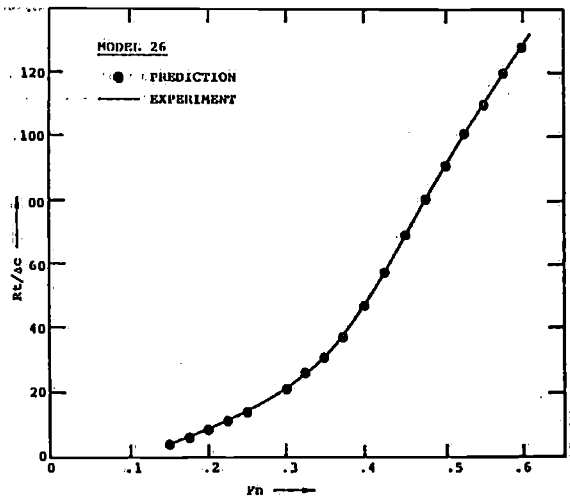

Figure 5b. Total upright resistance

TABLE 6

Residuary resistance polynomial coefficients
Fn = 0.45-0.60.

Fn	C_0	C_1	C_2	C_3	C_4
0.45	111.4237	-18.61120	-4.000404	1.667833	0.0033438
0.475	177.7123	-35.02741	-6.845442	3.290199	0.0057676
0.50	328.9239	-88.22548	-11.63294	9.258911	0.0107600
0.525	354.1405	-87.10124	-13.67890	8.638060	0.0124530
0.55	428.1995	-111.7306	-15.83484	11.29797	0.0145840
0.575	446.7202	-113.0711	-16.86441	11.21449	0.0155530
0.60	451.8823	-109.3091	-17.53909	10.55425	0.0160890

determine the relation between the heeled resistance, R_φ, the side force, F_h, the heel angle, φ, and the leeway angle, β, for a speed range corresponding to Fn = 0.27 to 0.45 and for a range of initial stabilities.

During each test run, the leeway angle was varied to obtain an equilibrium condition corresponding to combinations of Fn, φ, β, and GM, as described in reference [1]. The test conditions included Froude numbers from 0.271 to 0.452 and heel angles from 0 to 30 degrees. As in the Series I experiments, the trim moment due to the driving sail force and the heel moment due to the heeling side force were applied by shifting weights in the model. In addition, the vertical component of the sail force is taken into account by adding a weight at the longitudinal position of the centre of effort of the sail force.

The experimental data have been used to determine polynomial expressions for the leeway angle and the heeled resistance, as a function of heel angle, side force, wetted area and for the stability moment as a function of heel angle, displacement, length, vertical location of the centre of gravity and Froude number.

Heeled resistance

The difference between the heeled resistance R_φ and the total upright resistance, R_t, is split up into parts due to the side force production, to the induced resistance, and to a resistance component at zero side force which is, in turn, due to the change of the submerged part of the hull with heel and leeway.

For Series II, a satisfactory expression for the resistance increase is given by:

$$(R_\varphi - R_t)/qS_c = (C1 + C2*\varphi^2 + C3*Fn)*F_h^2/(qS_c)^2 + C4*Fn^2*\varphi \qquad (6)$$

where:

φ = heel angle in radians

S_c = wetted area of the canoe body

q = dynamic pressure = $\frac{1}{2}\rho V^2$

Table 7 contains the coefficients C for the six models of Series II.

TABLE 7

Coefficients C for heeled resistance

Model	C1	C2	C3	C4 * 10^3
23	0.524	0.931	4.912	17.04
24	-0.388	9.815	8.300	37.13
25	0.467	3.391	4.100	28.40
26	-0.355	15.446	7.460	38.96
27	0.820	1.180	0.712	17.66
28	-1.506	6.019	10.940	21.92

The mean rms error of the approximation is 0.2N (model values), which corresponds to slightly more than 1% of the upright resistance at hull speed.
For the hull forms with a large beam/draught ratio, the free surface effects due to side force production at large heel angles are important. The inclusion of Fn-dependent terms in (6) is necessary to obtain a satisfactory agreement with the measured resistance. In Figure 6 the goodness of fit of (6) to the experimental data is demonstrated for the Models 25, 26 and 27. For Model 27, with B_{wl}/T_c = 2.46, the free surface effects are relatively small as compared with those for Models 25 and 26.

Leeway

The leeway angle can be expressed by:

$$\beta = (F_h\cos\varphi/qS_c)*(B0 + B2*\varphi^2) + B3*\varphi^2*Fn \qquad (7)$$

where: φ and β are in radians, and $F_h\cos\varphi$ is the horizontal component of the side force.

The second term in (7) has to be included, because of the important assymetry of the underwater part of the canoe body, see Figure 7a. Note that, for the condition of no side force when heeled, the leeway angle will be:

$$\beta = B3 * \varphi^2 * Fn$$

For the series I models, the regression model (7) with B3 = 0 gave a satisfactory fit to the experimental data. For Model 27, with B_{wl}/T_c = 2.46, a similar approach for heel angles up to 20 degrees could be used, as shown in Figure 7b.

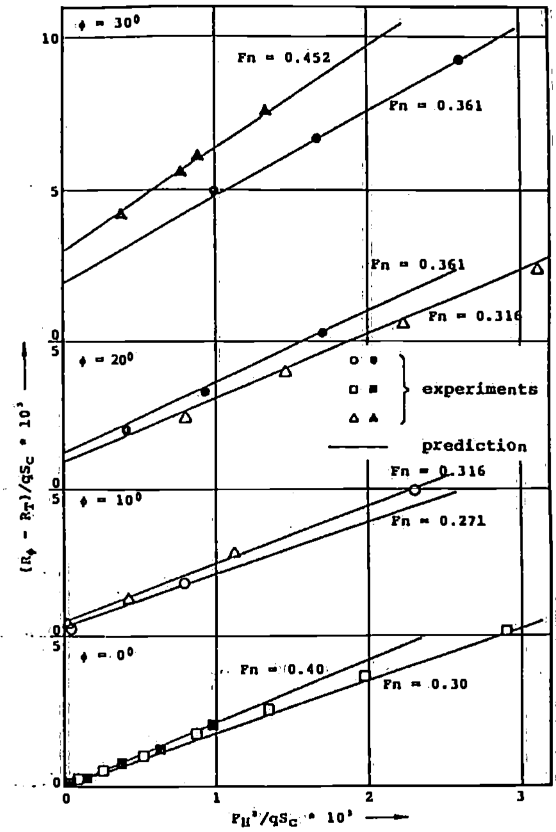

Figure 6a. Heeled resistance Model 25.

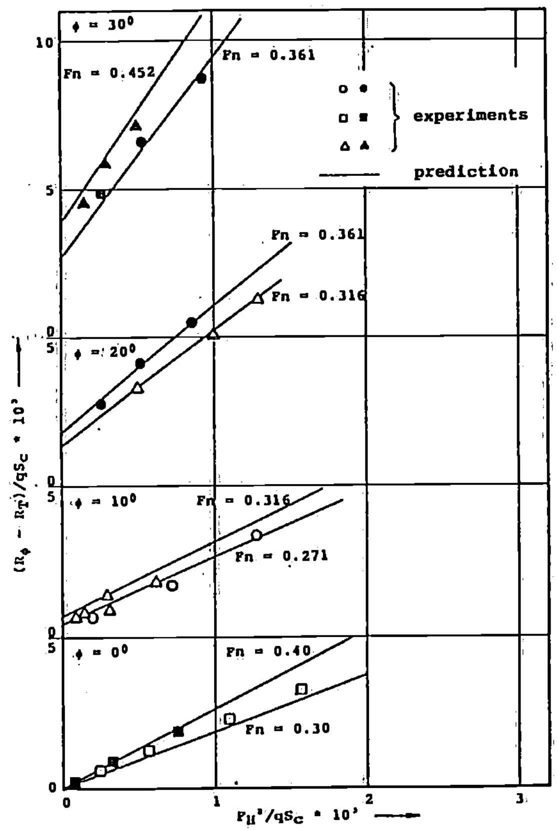

Figure 6b. Heeled resistance Model 26.

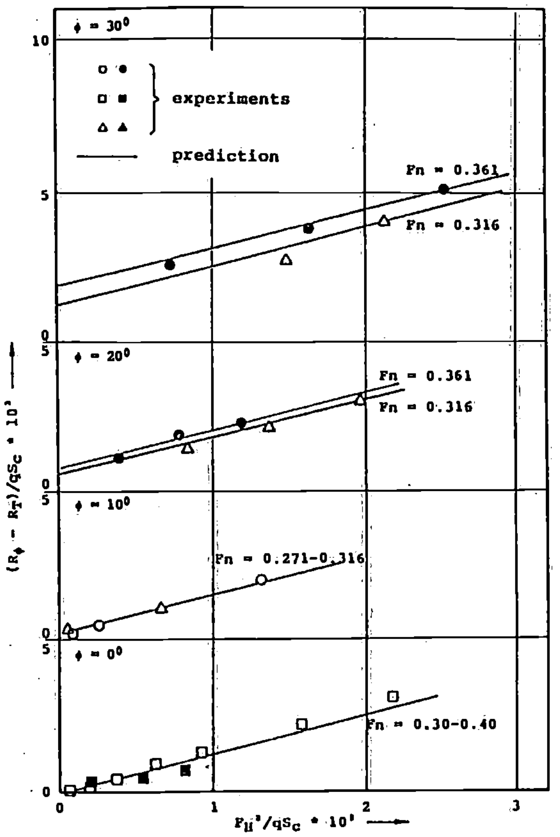

Figure 6c. Heeled resistance Model 27.

However the wide beam, very light displacement Model 26 clearly demonstrates the need of the additional term in (7).
In Table 8 the coefficients B of equation (7) are given for the six models.

TABLE 8
Coefficients B for the leeway-side force equation

Model	B0	B2	B3
23	3.080	2.530	0.064
24	3.670	9.094	0.302
25	2.889	4.949	0.110
26	3.362	8.552	0.842
27	2.291	1.237	0.110
28	2.886	5.785	0.272

The mean error of the least-squares fit is 0.3 degrees. The test conditions as analysed in this case are restricted to leeway angles smaller than 10 degrees in order to avoid unrealistic combinations of forward speed, heel angle and leeway.

Stability

The runs with a heel angle were used to determine the stability at forward speed. The analysis of the experimental data has been carried out as described in detail in reference [1].

The expression for the stability moment is given by:

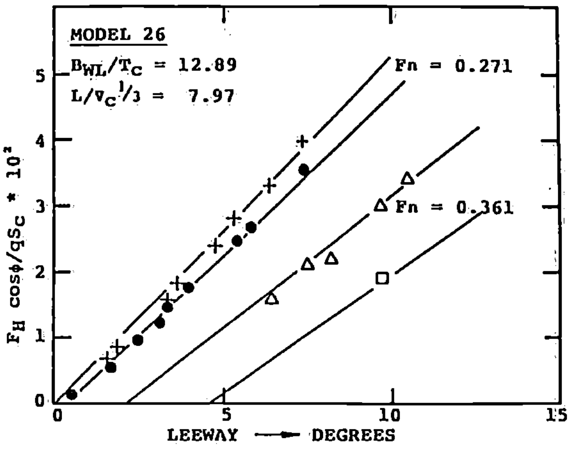

Figure 7a. Leeway-sideforce for Model 26.

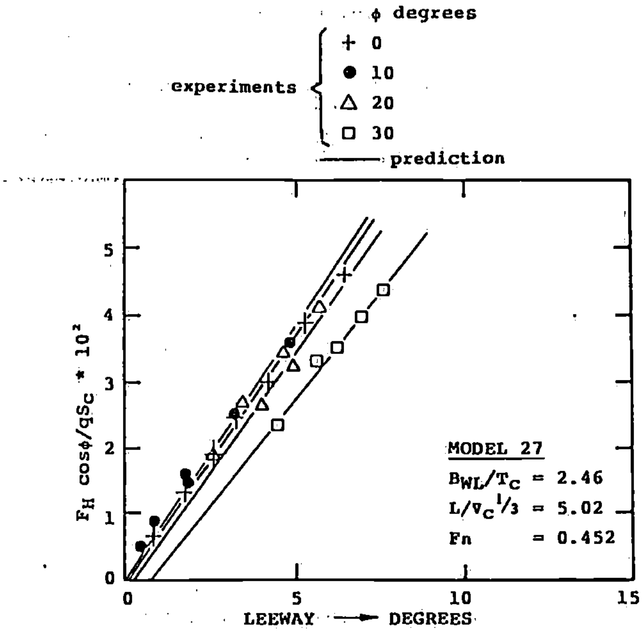

Figure 7b. Leeway-sideforce for Model 27.

$$Mst = \Delta_c * L_{wl} (D1*\varphi + D2*\varphi*Fn + D3*\varphi^2) + +\Delta z_G \sin\varphi \quad (8)$$

where: Δ_c = weight of displacement of the canoe body

Δ = weight of total displacement

z_G = distance of G with respect of the DWL, with positive being downward (below the DWL)

The centre of lateral resistance is located at a distance D4 * L_{wl} under the DWL and the heeling moment, M_h, follows from:

$$M_h = F_h (z_{CE} + D4 * L_{wl}) \quad (9)$$

where: z_{CE} is the distance of the centre of effort above the DWL in the upright condition.

The coefficients D are given in Table 9 for the six models of Series II.

TABLE 9

Stability and heeling moment coefficients D.

Model	D1	D2	D3	D4
23	0.086	0.010	-0.032	-0.066
24	0.212	0.073	-0.225	-0.041
25	0.102	-0.001	-0.052	-0.051
26	0.278	-0.193	-0.212	-0.048
27	0.013	-0.010	+0.012	-0.077
28	0.109	-0.010	-0.078	-0.072

For zero speed of advance and very small heel angles, it follows from (8) that:

$$\Delta_C * L_{wl} * D1 * \varphi = OM * \Delta * \varphi \quad (10)$$

where O is situated at the DWL.

Thus:

$$OM = \frac{\Delta_C}{\Delta} * L_{wl} * D1$$

and:

$$GM = \frac{\Delta_C}{\Delta} * L_{wl} * D1 + z_G \quad (11)$$

The stability lever has been calculated with equation (8), assuming a realistic position of the centre of gravity G for Models 25, 26 and 27, for Fn = 0.30 with φ = 10 degrees, and for Fn = 0.35 with φ = 20 and 30 degrees.

In Figure 8, the results are compared with hydrostatic calculations. Apparently, the very light wide-beam Model 26 loses stability due to dynamics effects, at forward speed.

From Table 9, it follows that the vertical position of the centre of lateral resistance is located between 30% and 50% of the total draught for the considered hull form and keel-rudder combinations.

PERFORMANCE PREDICTION

To show the effect of the length-displacement ratio on performance velocity, predictions based on the derived polynomial equations have been carried out.

To this end, three of the considered hull forms had to be transformed to actual designs. The same procedure has been followed as described in Reference [2], based on design data supplied by E.G. van de Stadt & Partners bv. In this procedure, a specific weight per unit hull volume has been chosen, ranging from 400 N/m^3 for the light model to 650 N/m^3 for the heavy model. This excludes the weight of the keel, but includes interior, fitting out and rigging. The vertical position of the centre of gravity of the hull and rig, without keel, has been assumed at 80% of the depth of the canoe body. The difference between this calculated weight and the total weight or displacement of a particular model yields the ballast weight. This ballast has been located in the keel, by filling the keel volume starting from the tip to the root as far as needed. The balast weight and its centre of gravity combined with the

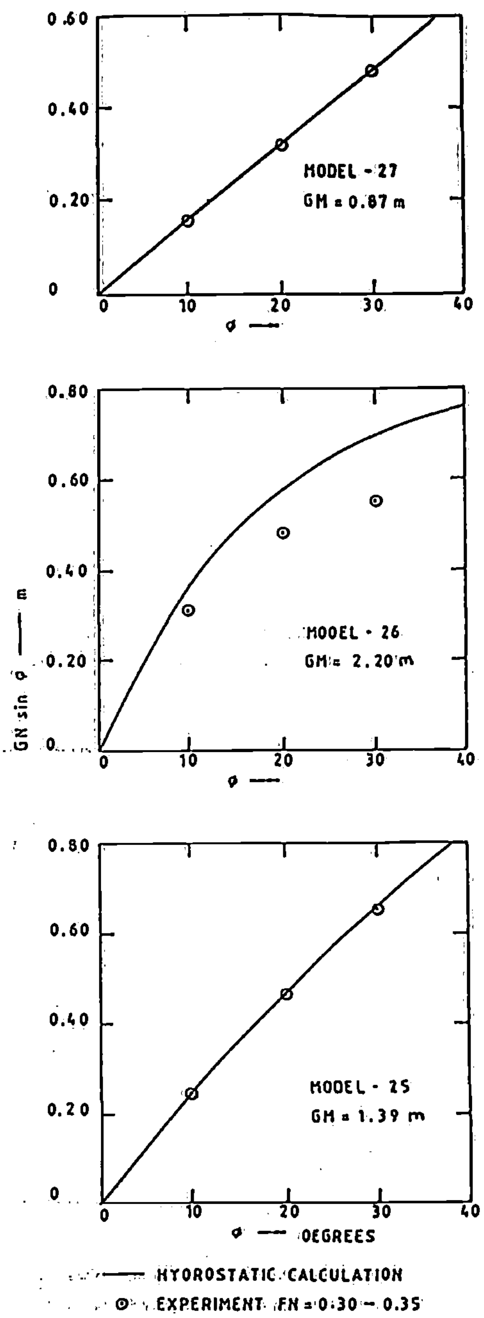

FIG. 8 Comparison of hydrostatic stability calculation with equation (8).

weight of hull and rig and its centre of gravity yielded the vertical centre of gravity of the combination. In this way, the realistic stability of the considered hull forms could be determined.

The sailplan dimensions followed from an assumed ratio of the sail area moment and the stability moment at 30 degrees of heel, based on practical experience with existing designs.

These considerations have led to the following main particulars for the Hull Forms 25, 26 and 27, with a nominal waterline length, L_{wl} of 10 meters, see Tabel 10.

TABLE 10

		Model		
		25	26	27
V	(m^3)	5.310	2.670	8.610
S	(m^2)	27.140	28.130	29.890
GM	(m)	1.630	2.390	1.150
RM	(Nm)	1482	1093	1695
I	(m)	13.800	11.300	15.750
J	(m)	4.600	3.770	5.750
P	(m)	12.350	9.850	14.300
E	(m)	3.530	2.810	4.090
B_{AD}	(m)	1.000	1.000	1.000
F_{MI}	(m)	0.860	0.860	0.860
S_A	(m^2)	53.500	35.100	74.500
S/S_A		1.970	1.250	2.480

$S_A = (I * J + P * E)/2$

TABLE 11

Performance of the three yachts at $V_{TW} = 10$ and $V_{TW} = 20$ knots.

Model nr.	true wind angle (degr)	appt. wind angle (degr)	speed (kn)	heel angle (degr)	speed ratio *
VTW = 10 knots					
25 medium	40	24	6.07	11	1.00
	60	33	7.34	12	1.00
	90	50	7.59	14	1.00
	120	75	6.93	4	1.00
	180	180	4.23	0	1.00
26 light	40	25	5.48	6	0.90
	60	34	7.22	7	0.98
	90	50	7.64	8	1.01
	120	77	6.42	1	0.93
	180	180	3.79	0	0.90
27 heavy	40	24	6.20	14	1.02
	60	33	7.23	18	0.99
	90	50	7.42	20	0.98
	120	75	6.96	7	1.00
	180	180	4.45	0	1.05
VTW = 20 knots					
25 medium	40	27	7.37	21	1.00
	60	39	8.16	29	1.00
	90	62	8.52	28	1.00
	120	87	9.08	18	1.00
	180	180	7.39	0	1.00
26 light	40	28	7.39	14	1.00
	60	40	8.49	20	1.04
	90	62	9.13	18	1.07
	120	87	9.95	12	1.10
	180	180	7.20	0	0.97
27 heavy	40	27	7.13	24	0.97
	60	38	7.77	32	0.95
	90	63	8.00	31	0.94
	120	84	8.43	23	0.93
	180	180	7.35	0	0.99

* speed ratio is (speed of Model-)/(speed of Model 25)

The rather extreme values of displacement and stability of Model 26, when brought to real scale, should be noted. In practice these values could be very difficult to achieve.
Using these data, a performance prediction has been made for the three designs at two different wind speeds, i.e., 10 and 20 knots true wind, using a velocity prediction program based on the new polynomial expressions for resistance, side force and induced resistance as given in equations (6), (7) and (8). The results for a limited number of true wind angles are presented in tabular form, since the polar plots show too litle detail, see Table 11.
From these results it may be concluded that the three designs attain more or less the same up-wind speed at $V_{TW} = 20$ knots, at which speed the heel angle may be 30 degrees or more in case of the heavier design (27). The lightest boat has smaller heel angles, but has considerably reefed and flattened her sail in this condition, to reduce heeling and thus reduce the associated large increase of the induced resistance for this hull form (with a large beam-draught ratio).
When reaching with $V_{TW} = 30$ knots, the lightest yacht has a speed which is upto 1.5 knots greater than that of the heavier, low beam-draught ratio yacht. The down wind speed is approximately the same.
At the 10 knot true wind speed, the lightest yacht goes significantly slower upwind, as is also the case in the downwind sailing condition. When reaching, the yachts have an almost identical performance; however, the light yacht tends to be slower as the reach becomes broader. Of particular interest is the optimum heel angle of the three different designs, as calculated by the velocity prediction program. In the calculation procedure, an optimisation routine is used to find the optimum speed as a function of the heel angle, by reefing and flattening of the sails [3]. It is clearly shown that the light yacht with the large beam-draught ratio and a corresponding steep increase in induced resistance due to heel performs best with the relatively small heel angles of 14 to 18 degrees, whereas the heavier yacht with the small beam-draught ratio may easily heel 30 or more degrees at optimum speed. The relatively poor performance of the light, large beam-draught yacht at the lower wind speed may be largely due to the relatively small sail-area/wetted-area ratio, which is typical for these designs.
The rather good all round performance of Model 25, the parent of Series II, is evident.
These results correspond reasonably well with experience on the race course.

The importance of stability may be demonstrated by the following results of a velocity prediction calculation in which, for all three designs, the GM value has been subsequently increased and decreased by 15% with respect to the original values as given in Table 12. Only the results for upwind and reaching are presented.

TABLE 12

Change in performance due to decreasing or increasing stability.

		VTW = 10 knots						
		-15%		original		+15%		
Model nr.	wind angle	speed	heel	speed	heel	speed	heel	speed ratio *
25	40	5.98	12	6.07	11	6.14	10	1.03
	60	7.29	14	7.34	12	7.37	10	1.01
	90	7.53	16	7.59	14	7.63	12	1.01
26	40	5.41	7	5.48	6	5.52	5	1.02
	60	7.12	8	7.22	7	7.52	4	1.06
	90	7.55	10	7.64	8	7.70	7	1.02
27	40	6.08	18	6.20	16	6.28	15	1.03
	60	7.17	21	7.23	18	7.27	16	1.01
	90	7.36	23	7.42	20	7.47	18	1.01
		VTW = 20 knots						
25	40	7.19	12	7.37	21	7.49	20	1.04
	60	7.97	29	8.16	29	8.35	28	1.05
	90	8.32	26	8.52	26	8.71	27	1.05
26	40	7.15	14	7.39	14	7.59	14	1.06
	60	8.27	18	8.49	20	8.84	18	1.07
	90	8.78	18	9.13	18	9.44	18	1.08
27	40	6.97	26	7.13	28	7.24	26	1.04
	60	7.63	32	7.77	32	7.89	32	1.03
	90	7.87	32	8.00	31	8.12	31	1.03

* speed ratio (speed with +15%)/(speed with -15%)

The yacht speed in these conditions, for all three designs, increases with increasing stability, although the effect lessens with increasing displacement; however, the increase in stability is supposed to be established without an increase displacement. In particlar, the model with the lowest displacement benefits most of an increase in stability, as may be concluded from these results (Model 26 has the largest relative speed increase with respect to the original values). This stresses the importance of adequate stability for Ultra Light Displacement Boats, a factor which may be difficult to accomplish in the search for light displacement.

REFERENCES

[1] Gerritsma, J., J.A. Keuning and R.Onnink
Geometry, Resistance and Stability of the Delft Systematic Yacht Hull Series.
5th HISWA Symposium, Amsterdam, 1981.

[2] Gerritsma, J. and J.A. Keuning
Performance of Light- and Heavy-Displacement Sailing Yachts in Waves.
South East Section of the Society of Naval Architects and Marine Engineers
St. Petersburg, Florida, 1988.

[3] Kerwin, J.E.
A Velocity Prediction Program for Ocean Racing Yachts.
New England Sailing Symposium, New Londom Connecticut, 1976.